T2R2 東京科学大学 リサーチリポジトリ
Science Tokyo Research Repository

論文 / 著書情報
Article / Book Information

Title	Optimization of a two-step biodiesel production from waste cooking oil: Comparative evaluation of n-hexane and CPME as transesterification cosolvents
Authors	Md. Rubel, Cheng Shuo, Sasipa Boonyubol, M.M. Harussani, Surendra Singh Kachhwaha, Jeffrey S. Cross
Citation	Chemical Engineering Research and Design, Vol. 226, , Page 282-295
Pub. date	2026, 1
DOI	https://dx.doi.org/10.1016/j.cherd.2026.01.005
Creative Commons	Information is in the article.

Powered by T2R2 (Science Tokyo Research Repository)

Chemical Engineering Research and Design 226 (2026) 282–295

Contents lists available at ScienceDirect

Chemical Engineering Research and Design

journal homepage: www.elsevier.com/locate/cherd

Optimization of a two-step biodiesel production from waste cooking oil: Comparative evaluation of n-hexane and CPME as transesterification cosolvents

Md. Rubel [a,*], Cheng Shuo [a], Sasipa Boonyubol [a], M.M. Harussani [a], Surendra Singh Kachhwaha [b], Jeffrey S. Cross [a,*]

[a] Department of Transdisciplinary Science and Engineering, School of Environment and Society, Institute of Science Tokyo, 2-12-1 Ookayama, Meguro-ku, Tokyo 152-8550, Japan
[b] Centre for Biofuels and Bioenergy Studies, School of Technology, Pandit Deendayal Energy University, Gandhinagar, Gujarat 382426, India

ARTICLE INFO

Keywords:
Biodiesel
Waste cooking oil
Acid-base catalysis
Cosolvent
Renewable energy
Carbon neutrality

ABSTRACT

Biodiesel derived from waste cooking oil (WCO) represents a promising strategy for meeting energy demands, mitigating environmental impact, and supporting carbon neutrality goals in countries such as Japan and India. However, conventional alkaline transesterification faces challenges, including soap formation from free fatty acids (FFAs) in WCO and poor miscibility of oil and alcohol phases, both of which limit efficiency. Although one-step acidic esterification and traditional organic cosolvents have been explored to overcome these drawbacks, such approaches raise economic and environmental concerns. Thus, this study investigated a two-step acid-base catalysis process employing the low-toxicity cyclopentyl methyl ether (CPME) cosolvent for the production of biodiesel from WCO, which was collected from local restaurants in Tokyo, Japan. The process was carried out through initial acidic esterification to convert FFAs to esters, followed by alkaline transesterification optimized at a 1:6 oil-to-cosolvent molar ratio. CPME, characterized by its low toxicity, intermediate polarity and excellent miscibility, facilitated a high biodiesel yield of 97.5 %, outperforming n-hexane (96 %) and reactions conducted without a cosolvent (89 %). Gas chromatography-mass spectrometry (GC-MS) analysis confirmed that the synthesized biodiesel met the EN 14214 European quality standard (≥96.5 % FAME content). The process operated at a mild temperature of 40°C, enhancing yield with lower energy input. Overall, the CPME-assisted two-step process offers an efficient and viable route for biodiesel production from waste feedstocks.

1. Introduction

Global energy consumption is projected to increase by 15 % from 2021 levels, reaching 660 quadrillion Btu by 2050 (ExxonMobil. ExxonMobil, 2024). Japan's energy consumption for 2050 is anticipated to reach 20 quadrillion Btu, driven by population dynamics, technological advancements, and economic growth (Ministry of Economy, 2015). Moreover, Japan's heavy reliance on fossil fuels raises significant concerns about emissions, underscoring the urgent need for a carbon-neutral energy solution (Ambat et al., 2020). To address these concerns, during the 26th Conference of the Parties (COP26), Japan pledged to achieve net-zero emissions by 2050, aiming to reduce emissions by 46 % by 2030 compared with 2013 levels (Ministry of Economy, 2015; The National Bureau of Asian Research. The National Bureau of Asian Research, 2023). Similarly, India, the third-largest emitter of carbon dioxide (CO_2), experienced a 6 % increase in emissions in 2022 and plans to decrease emission intensity by 45 % by 2030 while attaining net-zero emissions by 2070 (Midha and Tomar, 2023). Achieving these objectives requires a rapid transition to clean and renewable energy sources, reducing dependence on nonrenewable energy (Bai et al., 2022). In this context, renewable energy sources, including solar, wind, hydro, and biodiesel, offer viable alternatives for minimizing environmental impact and advancing toward a decarbonized society (Singh et al., 2017). Among these options, biodiesel stands out as a promising alternative due to its biodegradability, nontoxicity, renewability, and reduced sulfur and CO emissions compared to conventional diesel (Khan et al., 2020; Najaf-Abadi et al., 2024; Paryanto et al., 2019; Thushari and Babel, 2018; Baskar et al., 2018; Liu et al.,

* Corresponding authors.
E-mail address: office-cross@tse.ens.titech.ac.jp (J.S. Cross).

https://doi.org/10.1016/j.cherd.2026.01.005
Received 12 October 2025; Received in revised form 27 November 2025; Accepted 4 January 2026
Available online 5 January 2026
0263-8762/© 2026 The Author(s). Published by Elsevier Ltd on behalf of Institution of Chemical Engineers. This is an open access article under the CC BY-NC-ND license (http://creativecommons.org/licenses/by-nc-nd/4.0/).

2024). Additionally, studies indicate that blending up to 20 % biodiesel with diesel is compatible with most engines (Bhatia et al., 2021). Furthermore, transesterification remains an economical and efficient process for biodiesel synthesis, generating biodiesel as the main product and glycerol as a valuable byproduct (Chilakamarry et al., 2021; Moklis et al., 2024, 2023). The two-step acid-base catalysis provides additional advantages, such as enhanced yield, reduced corrosion, shorter reaction times, and minimal soap production (Ali and Fadhil, 2013; Maddikeri et al., 2012; Grosmann et al., 2022).

Moreover, the primary challenge in biodiesel production is the high cost of raw materials, which account for nearly 80 % of total production costs. While edible oils (vegetable, animal oils, and fats) are commonly used (Altikriti et al., 2015), non-edible oils (e.g., castor oil) (Fadhil et al., 2020; Hassan and Fadhil, 2025), waste oils (Girish et al., 2013; Gouran et al., 2021; Mohadesi et al., 2022), and microalgae offer promising alternatives to edible oils. Nonetheless, their cost competitiveness is limited and often reliant on government subsidies (Bart et al., 2010). The insufficient self-sufficiency of oils and fats in Japan and India renders biodiesel production from edible oil unfeasible (Cai et al., 2015; Statista Inc, 2023, 2023; Parija, 2022). By contrast, waste cooking oil (WCO) represents a financially viable option, as Japan disposes of 400, 000 tons and India 3 million tons annually. WCO supports a circular economy, mitigates edible oil supply issues, and is fundamentally cost-free, adhering to biodiesel feedstock criteria while substantially lowering feedstock expenses (Cai et al., 2015; The Asahi Shimbun Company, 2024; India's WCO, 2023). Thus, this research regarded WCO as a suitable biodiesel feedstock.

Despite these benefits, the characteristics of WCO, including the acid value (AV) and moisture content, influence biodiesel production yields (Mohadesi et al., 2022). The elevated free fatty acid (FFA) concentration in WCO hinders one-step alkaline transesterification, resulting in soap production and decreased yields due to inadequate reactant miscibility (Salleh et al., 2023; Mićić et al., 2019). To optimize the alkaline transesterification process, a trial-and-error experimental approach was employed. However, few studies have focused on enhancing the deacidification of FFAs during the preliminary esterification phase. Furthermore, mass transfer between oil and methanol phases also significantly influences the reaction rate in the alkaline transesterification process. Although elevated temperatures increase solubility, they increase energy consumption, with biodiesel output rising by only 2–3 wt% for every 10°C increment (Ma et al., 1998).

A promising solution to these challenges is the cosolvent approach, which enhances the solubility of oil and methanol at reduced temperatures, thereby lowering energy consumption and enabling solvent recovery and reuse (Jin et al., 2020). Early studies have investigated various cosolvents, including acetone (Encinar et al., 2016; Okitsu et al., 2013; Kanna, 2018; Julianto and Nurlestari, 2018), diethyl ether (DEE), dibutyl ether (diBE), tert-butyl methyl ether (tBME), diisopropyl ether (diIPE), tetrahydrofuran (THF) (Encinar et al., 2016), and hexane (Muppaneni et al., 2015), to address the immiscibility challenges in biodiesel production from WCO. Among these, n-hexane is favored due to its hydrophobic nature and low boiling point (Bai et al., 2022), which facilitates biodiesel production at lower operating temperatures (Jin et al., 2020; de Gonzalo et al., 2019; Simonelli et al., 2020; Lamatinulu, 2022). However, the volatility and toxicity of these solvents in high-FFA feedstocks like WCO (>2 % FFA) pose environmental and safety risks, highlighting the need for safer alternatives (Cerón Ferrusca et al., 2023). The high volatility of organic solvents improves separation efficiency, but also increases flammability, toxicity, and health hazards, requiring costly safety and recovery measures (Taher and Al-Zuhair, 2017). In response to these limitations, cyclopentyl methyl ether (CPME) has been identified as an environmentally benign cosolvent with significant advantages over other solvents, such as 2-methyltetrahydrofuran (2-MeTHF) and 1,8-diazabicycloundec-7-ene (DBU). While, 2-MeTHF is a common alternative, it is prone to hygroscopicity (absorbing moisture) and presents a potential for peroxide formation (Pace et al., 2012). Similarly, deep eutectic solvents (DES) are often explored as potential alternatives but frequently exhibit high viscosity, which constrains mass transfer and typically results in lower biodiesel yield (Smith et al., 2014). In contrast, CPME's low peroxide formation, low flammability, reduced toxicity, and safe recovery make it a promising alternative (de Gonzalo et al., 2019; Taher and Al-Zuhair, 2017). Moreover, CPME is classified as a green solvent due to its low toxicity, high chemical stability, safety (low peroxide formation and higher flash point), environmental benefits (high reusability, low wastewater generation), and process efficiency. Additionally, the main difference between bio-based and synthetic CPME lines is in their source: synthetic CPME is petrochemical-based, while bio-based CPME is derived from renewable biomass, making it more viable with a lower carbon footprint (de Gonzalo et al., 2019; Taher and Al-Zuhair, 2017; Sakamoto, 2013; Watanabe, 2013). Furthermore, with a dielectric constant of 4.76, dipole moment of 1.27, and polarity index of 2.8, CPME effectively reduces immiscibility in high-FFA WCO feedstocks. Despite these promising properties, its application in biodiesel synthesis from WCO remains underexplored (Joorasty et al., 2022) (De Jesus et al., 2020).

This study aims to fill this gap by developing a cost-effective and efficient method for biodiesel production from high FFA feedstocks, specifically WCO. We applied a two-step acid-base catalytic process, including acidic esterification to convert FFAs, followed by optimized alkaline transesterification (Process-I), as illustrated in Fig. 1. This approach leads to a reduction of soap formation and increases biodiesel yield. Importantly, the study introduces CPME as a novel, low-toxicity cosolvent to enhance miscibility and mitigate mass transfer resistance during the transesterification reaction. Crucially, we employed a hierarchical approach: after optimizing the baseline alkaline transesterification process (Process-I), we applied these optimal conventional conditions to the cosolvent systems (Process-II with n-hexane and Process-III with CPME) to specifically quantify the direct performance enhancement attributable to the cosolvent. The comparative analysis of fatty acid methyl ester (FAME) profiles highlights CPME's superiority as an environmentally friendly alternative and a reaction intensifier. Therefore, the findings of this study could have a substantial impact on the future of biodiesel production, particularly in regions where WCO is abundant, offering a scalable solution to global energy and environmental challenges.

2. Materials and methods

2.1. Materials

The WCO sample used in this study was collected from local restaurants as the primary feedstock in Ookayama, Meguro-ku, Tokyo, Japan, which was initially sourced from BBQ edible oil, manufactured by Youngmi Co., Ltd. in Korea. The nutritional profile of the fresh oil included 14 g of total fat (22 % daily value (DV)), 2 g of saturated fat (10 % DV), 6 g of polyunsaturated fat, and 5.5 g of monounsaturated fat, with no detectable cholesterol, sodium, carbohydrate, or protein. Notably, due to repeated use in high-temperature frying, the collected WCO contained visible solid impurities.

2.2. Chemicals

All chemicals and reagents used in this study were of analytical grade and were procured from Fujifilm Wako Pure Chemical Industries, Osaka, Japan. The reagents included methanol (MeOH, 99.8 %), sulfuric acid (H_2SO_4, 95 %), potassium hydroxide (KOH, 85 %). The cosolvents evaluated were n-hexane (Wako 1st grade), and CPME (99 %). In contrast to the WCO feedstock, the cosolvents n-hexane and CPME were utilized as supplied chemical reagents. Notably, no further purification was conducted before their use.

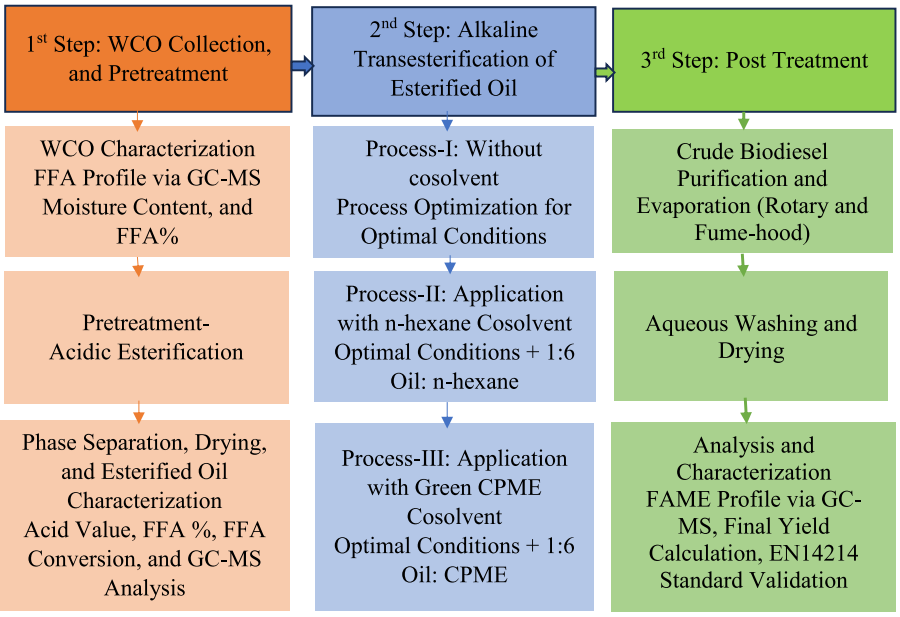


Fig. 1. Schematic workflow of biodiesel production from WCO via a two-step acid-base catalytic process. The methodology involves pre-treatment of acidic esterification to reduce FFA content, followed by alkaline transesterification under optimized conditions without a cosolvent (Process-I), with n-hexane (Process-II) and CPME (Process-III) cosolvents at a 1:6 oil: cosolvent ratio.

2.3. Preparation of the WCO sample

The WCO sample contained residual food particles and moisture (H_2O) resulting from the frying process, which were carefully removed before the esterification and transesterification reactions. Initially, the collected WCO was allowed to settle at room temperature for 4–6 days (Degfie et al., 2019). Subsequently, the oil underwent a sequential four-step filtration procedure, starting with gravity filtration using 110 mm filter paper, followed by Linicon LV-125A vacuum filtration (Nitto Kohki Co., Ltd., Japan) through a 10 µm membrane and finally through 0.8 µm and 0.5 µm filter papers. This sequential filtration effectively eliminated food residues, additives, and various impurities. Detailed schematics of the filtration protocol are provided in Fig. S1.

2.3.1. Pretreatment of WCO

Prior to the esterification reaction, the filtered WCO sample was pretreated by heating at 100–110°C for 1 h to reduce the moisture content effectively (Emmanouilidou et al., 2024). To prevent hydrolysis and prevent any increase in FFA levels, the oil was stirred continuously using a magnetic stirrer at 100–150 rpm. This stirring not only minimized hydrolysis but also facilitated the evaporation of H_2O, thereby accelerating the pretreatment process. An illustration of this pretreatment procedure is provided in Fig. S2.

2.3.2. Derivatization of WCO for FFA profile determination

The frying process induces significant chemical and physical changes in the oil, including hydrolysis, polymerization, and oxidation, which lead to the formation of FFAs and H_2O. To characterize the FFA profile in the WCO, a derivatization method was employed. Specifically, 20 mg of oil was combined with 1 mL of a MeOH-H_2SO_4 mixture (2.5 % v/v–97.5 % v/v) in a beaker. The mixture was homogenized and then reacted at 80°C for 90 min. Following the reaction, 1.5 mL of an aqueous sodium chloride (NaCl) solution (0.9 %) was added to reduce the solubility of methyl esters in the oil phase. The sample was thoroughly stirred, and the FAMEs were subsequently extracted with 1.5 mL of analytical-grade n-hexane. Finally, the derivatized sample was analyzed via GC—MS to confirm the FFA profiles of the WCO sample (Guo et al., 2021).

2.4. Biodiesel synthesis

2.4.1. First step: experimental procedure for acidic esterification of WCO

The acidic esterification reaction was carried out in a 250-mL Erlenmeyer flask (Simax, Czech Republic) equipped with a magnetic stirrer and a cooking thermometer placed on a hot plate (As One, China). Throughout the reaction **(**Fig. 2**(a)),** the following parameters were maintained: 10 g of WCO, an oil to MeOH molar ratio of 1:10, an H_2SO_4 concentration of 5 wt% (de Gonzalo et al., 2019), a reaction time of 120 min, and a temperature of 60°C. Upon completion, the reaction mixture was transferred to a separating funnel and allowed to settle overnight. This resulted in two distinct phases: an esterified oil phase on top and an aqueous H_2O phase at the bottom containing residual MeOH, H_2SO_4, and H_2O **(**Fig. 2 **(b)).** To eliminate any residual MeOH and moisture from the esterified layer, drying was performed on a heating plate at 110°C for 15–20 min (Miyuranga et al., 2023). The conversion of FFAs to FAMEs was subsequently confirmed by GC—MS analysis and the esterified oil was stored for use in the subsequent alkali-catalyzed transesterification step.

2.4.2. Second step: experimental procedure for the transesterification of esterified WCO

The second step involved the transesterification of the esterified WCO using MeOH as a reactant and KOH as the catalyst **(**Fig. 2 **(c)).** This reaction was conducted in a 250 mL Erlenmeyer flask equipped with a magnetic stirrer and a cooking thermometer to facilitate biodiesel production. A series of experiments was performed to optimize four key process parameters**:** catalyst concentration (1–5 wt% KOH), oil-to-MeOH molar ratio (1:3–1:8), reaction temperature (35–60°C, in 5°C increments), and reaction time (15–90 min, at 15-min intervals). The optimal conditions were identified as: a 2 wt% KOH catalyst concentration, an oil-to-MeOH molar ratio of 1:6, a reaction temperature of 40°C, and a reaction time of 60 min. These optimized conditions, which resulted in the highest biodiesel yield and FAME content, were designated as Process-I. Throughout this optimization, the quantity of esterified WCO and the agitation rate (600 rpm) were kept constant.

Additionally, to enhance oil-to-solvent miscibility and mitigate mass transfer resistance, either n-hexane (Process-II) or CPME (Process-III) was introduced. For these cosolvent-assisted systems, all optimized

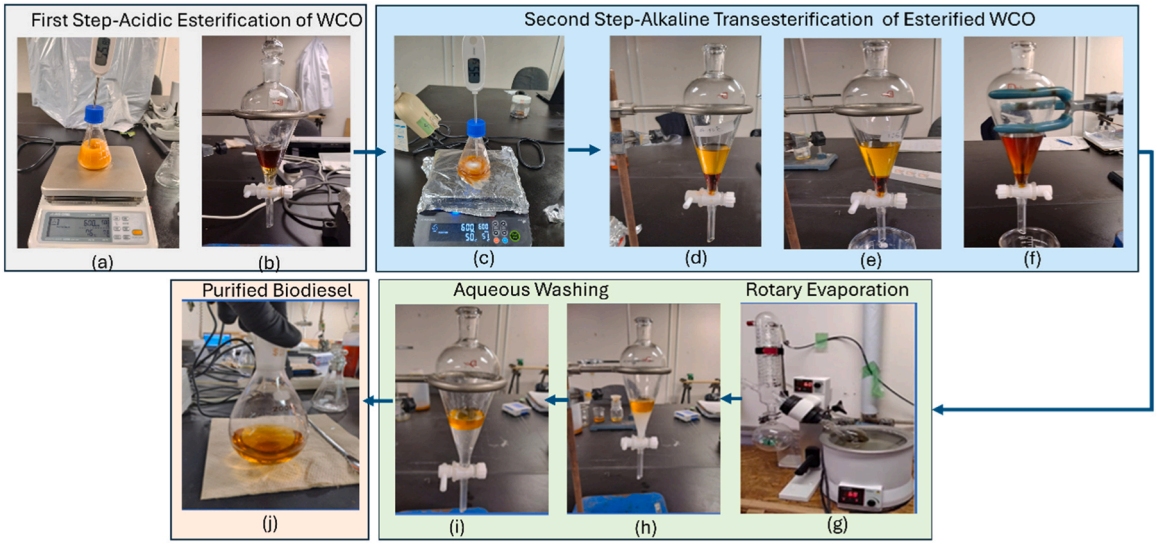


Fig. 2. Comprehensive workflow for biodiesel production from WCO via a two-step acid and base catalysis process with cosolvents. The first step is (a) acidic esterification of WCO, resulting in(b) esterified oil (top layer) and an aqueous phase (bottom layer). The second step is (c) alkaline transesterification of the esterified WCO under three distinct conditions: (d) Process-I (baseline without cosolvent), (e) Process-II (with an n-hexane) and (f) Process-III (with CPME cosolvent). In this step, the top layer represents biodiesel (FAME), and the bottom layer represents glycerol. Final purification includes (g) rotary evaporation and multiple cycles of aqueous washing:(h) first cycle and (i) sixth cycle, ultimately leading to (j) The purified biodiesel as the final product.

conditions established in Process-I (2 wt% KOH, 1:6 oil: MeOH, 40°C, and 60 min) were maintained, while the oil-to-cosolvent molar ratio was independently optimized for each solvent. Upon completion, the reaction mixture was transferred to a separating funnel and allowed to separate into two distinct phases (Fig. 2(d) for Process-I, Fig. 2(e) for Process-II, and Fig. 2(f) for Process-III). The upper layer consisted of biodiesel (FAME), whereas the lower layer comprised glycerol, catalyst residues, and unreacted MeOH (Emmanouilidou et al., 2024; Haq et al., 2021; Abidin et al., 2012). It is important to note that all transesterification experiments, including parameter optimization and cosolvent evaluations, were conducted in duplicate, with measurements at optimal conditions verified in triplicate to ensure reproducibility. Reported yields represent mean values with standard deviations. Table 1 provides a summary of the experimental conditions applied during this stage.

2.5. Post-treatment

Following the transesterification reaction, the mixture was transferred to a separating funnel and allowed to settle. The homogenous KOH catalyst, being soluble in the polar glycerol-methanol phase, was primarily removed during the initial separation of the bottom glycerol layer. Residual MeOH and n-hexane in the biodiesel sample were removed via rotary evaporation using a rotary evaporator oil bath (As One, Japan), whereas CPME was allowed to evaporate directly under the fume hood for the purification step. The biodiesel was then washed several times with distilled water, with the aqueous phase separated at each stage. Any residual catalyst remaining in the biodiesel phase was removed through these multiple cycles of aqueous washing, as shown in Fig. 2 **(g)-** 2**(j)**. Finally, the resulting biodiesel phase was dried at 100–110°C for 15–20 min to remove any remaining H_2O before GC—MS analysis.

Table 1
Summary of the second-step alkaline transesterification conditions for esterified WCO.

Parameters	Process-I (without cosolvent)	Process-II (with n-hexane cosolvent)	Process-III (with CPME cosolvent)
Catalyst (2 wt%)	KOH	KOH	KOH
Temperature (°C)	40	40	40
Oil to MeOH mole ratio	1:6	1:6	1:6
Reaction time (min)	60	60	60
Oil to cosolvent mole ratio	None	1:6	1:6
Agitation (rpm)	600	600	600

2.6. Analytical methods

2.6.1. Moisture content in WCO

After heating at 100–110°C, the H_2O content of the WCO sample was determined using Eq. (1) (Alias et al., 2018):

$$H_2O\ \text{content} = \frac{\text{Initial weight} - \text{Final weight}}{\text{Initial weight}} \times 100 \quad (1)$$

2.6.2. Determination of the FFA content in WCO

To quantify the FFA content in the WCO, 0.5 g of the sample was dissolved in 10 mL of ethanol, and 1–2 drops of phenolphthalein were added as indicators. The resulting mixture was titrated with 0.1 N NaOH until a persistent pink color appeared, indicating the titration endpoint (Sadaf et al., 2018). The FFA% of the esterified oil was determined using the same procedure, and the FFA % content was calculated using Eq. (2).

$$\text{FFA\%} = V \times N \times \frac{28.2}{W} \times 100 \quad (2)$$

Here, V (mL) denotes the volume of standard NaOH solution used to reach the titration endpoint, N represents the normality of the standard NaOH solution (0.1 N), and W (g) represents the weight of the WCO sample (0.5 g).

2.6.3. Determination of the acid value (AV) of esterified oil

Two grams of the esterified oil sample (2.4.2) were placed in a conical flask, to which 50 mL of a neutral alcohol-ether mixed solution was added for the determination of the AV of the esterified oil. The mixture was heated in a H_2O bath until the sample dissolved completely. After cooling to room temperature, 2–3 drops of phenolphthalein indicator were added. The solution was then titrated with 0.1 N KOH

standard solution until a persistent faint pink color was observed, lasting at least 30 s, indicating the titration endpoint (Guo et al., 2021). The AV was calculated using Eq. (3):

$$AV = V \times C \times \frac{56.1}{m} \quad (3)$$

where V (mL) is the volume of the standard KOH solution used to reach the titration endpoint.

C (mol/L) is the molar concentration of the KOH standard solution, 56.1 (g/mol) is the molecular weight of KOH, and m (g) is the weight of the test sample.

Additionally, detailed procedures for the analytical methods used in this study, including blank titration, FFA determination of WCO, and acid value calculation of the esterified oil, are provided in Fig. S3.

2.6.4. Determination of the FFA content in the esterified oil

Eq. (4) was used to calculate the FFA content of the esterified oil (Miyuranga et al., 2023).

$$FFA\% = \frac{\text{Acid value}(\text{mg}\frac{KOH}{g})}{2} \quad (4)$$

2.6.5. Determination of FFA conversion

The FFA conversion rate was calculated using Eq. (5) (Rahma and Hidayat, 2023).

$$\text{FFA Conversion} = \frac{\text{Initial FFA} - \text{Final FFA}}{\text{Initial FFA}} \times 100 \quad (5)$$

The initial and final FFA values are expressed as percentages (%), and the titration was performed via a burette, a titration flask, the sample to be titrated, and a ring stand.

2.6.6. Gas chromatography—mass spectrometry (GC—MS) characterization technique

GC—MS analysis was conducted to characterize the FFAs in the WCO, as well as the FAME compositions of both the esterified oil and the final biodiesel samples. The QP-2010 GC-MS (Shimadzu, Japan) was utilized, equipped with an Rxi-5Sil MS capillary column measuring 30 m in length × 0.25 mm in internal diameter and 0.25 μm in film thickness. GC—MS was utilized for both qualitative and quantitative analysis of liquid and gaseous molecules by integrating two complementary techniques: GC, which separates sample components, and MS, which detects and identifies molecules based on their mass-to-charge — (m/z) ratios and fragmentation patterns. An autosampler facilitated the injection of a 1 μL sample. The injector temperature was maintained at 200°C to ensure rapid vaporization of the analytes, while helium (He) served as the carrier gas at a flow rate of 1.5 mL/min. The oven temperature program comprised three stages tailored for different analyses: an initial hold at 80°C for 5 min, followed by an increase to 280°C at 5 °C/min for FAME analysis, then an increase to 320°C at 2.5 °C/min, and finally an increase to 350°C at 1 °C/min for triglyceride analysis.

The identification of chemical compounds were achieved by comparing the acquired mass spectra against reference spectra in the National Institute of Standards and Technology (NIST) library. This matching process involved evaluating both m/z — values and the characteristic fragmentation pattern to accurately determine the chemical composition of the sample.

2.6.7. Biodiesel yield analysis

Based on the GC—MS analysis results, the biodiesel yield (%) content was calculated using Eq. (6) (Prajapati et al., 2024).

$$\text{Biodiesel yield}(\%) = \frac{\text{Total biodiesel produced}(gm) \quad * \quad (\%\text{FAME from GC} - \text{MS})}{\text{Total oil used in reaction}(gm)} \text{x}100\ldots \quad (6)$$

3. Results and discussion

3.1. WCO characterization

The fatty acid profile of the WCO was analyzed via GC—MS (Fig. S4) and showed values consistent with published literature (A Zayed et al., 2016; Kumar et al., 2020; Di Pietro et al., 2020). The moisture content was determined to be 0.09 % based on Eq. (1), which aligns with previously published data (Taher and Al-Zuhair, 2017) (Al-Saadi et al., 2020). Furthermore, the GC—MS analysis results, presented in Fig. 3 and Table S1, revealed five major fatty acids by relative area: palmitoleic (1 %), palmitic (15.95 %), linoleic (33.35 %), oleic (41.69 %), and stearic acid (6.40 %), with molecular weights ranging from 268.4 to 298.51 g/mol. WCO generally has a similar fatty acid profile to fresh vegetable oil, but contains significantly higher levels of FFAs, moisture, food additives, and degradation byproducts due to repeated heating, oxidation, hydrolysis, polymerization, and exposure to air during the deep frying process, which is commonly practiced in local restaurants. This observation is consistent with previous studies (Abrante-Pascual et al., 2024; Mariana et al., 2020; Manzoor et al., 2022).

3.2. Esterification of WCO

The acid esterification of WCO was comprehensively assessed using the FFA conversion rate (a relative measure), the AV (an absolute measurement), and GC—MS analysis. The process achieved a 91.68 % conversion of FFAs, and reduced the FFA contents from an initial 10.7 % to 0.89 % under optimal conditions (5 wt% H_2SO_4, 60°C (de Gonzalo et al., 2019), an oil-to-methanol molar ratio of 1:10, agitation at 700 rpm, and a reaction time of 120 min), highlights the effectiveness of this process as a pretreatment step. The reduction of the initial FFA content to below 1 % (0.89 %) validates the suitability of the sample for subsequent alkali-catalyzed transesterification (Step-2). The measured AV of 1.78 mg KOH/g after esterification further supports successful deacidification. Additionally, the effect of MeOH on the esterification reaction was confirmed by the GC—MS chromatograms presented in Fig. S5 and Fig. S6, which demonstrated the conversion of FFAs to FAMEs. The GC—MS analysis results of esterification reaction, shown in Fig. 4 and Table S2, detail the FAME composition: methyl elaidate (trans) (65.76 %) and methyl linoleate (19.91 %) were the predominant components, followed by methyl palmitate (6.56 %), methyl oleate (cis) (4.41 %), and methyl stearate (3.36 %). Mechanistically, the reaction mechanism follows classical acid-catalyzed esterification theory, whereby H_2SO_4 acts as a proton donor, activating the FFA's carbonyl group to increase its electrophilicity and facilitate nucleophilic attack by methanol. This reversible reaction equilibrium was successfully shifted to favor FAME formation.

3.3. Impact of transesterification reaction parameters on biodiesel yield %

To evaluate the impact of the process parameters, specifically, the KOH catalyst loading, oil-to-MeOH molar ratio, reaction temperature, and reaction time, on the biodiesel yield, a systematic univariate study

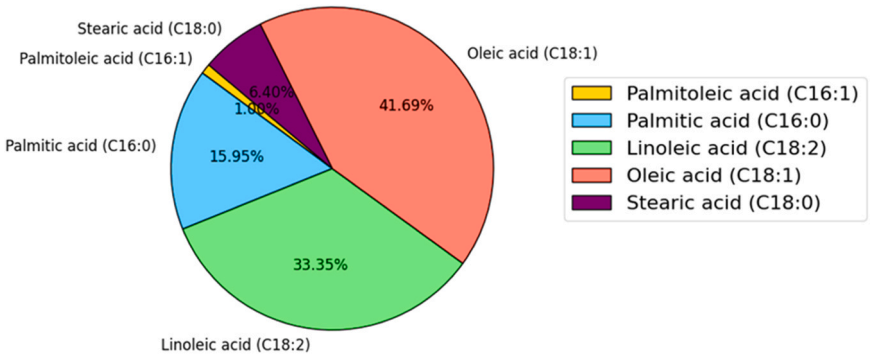


Fig. 3. Proportional distribution of major free fatty acid components in WCO.

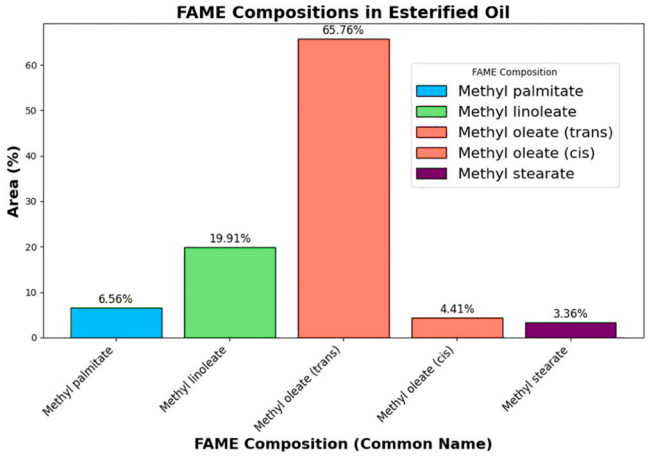


Fig. 4. FAME percentage compositions of the esterified oils.

was performed under controlled experimental conditions. Each parameter varied independently while keeping the remaining variables constant to ensure valid comparisons. The detailed impact of these parameter on the biodiesel yield are described in the following sections.

3.3.1. KOH catalyst loading

To evaluate the impact of catalyst concentration on biodiesel yield **(**Fig. 5**(a)),** a baseline reaction without a catalyst was conducted at 40°C for 60 min with an oil-to-MeOH molar ratio of 1:6, resulting in a 25 % yield**.** Subsequently, catalyst loadings ranging from 1 to 5 wt% KOH were tested under the same conditions. The biodiesel yield increased from 84 % to 89 % as the catalyst concentration was raised from 1 wt% to 2 wt%. However, further increases in catalyst loading to 3–4 wt% caused a decrease in yield, attributed to saponification due to excess KOH, which led to soap, glycerol formation, and complicated downstream purification (Degfie et al., 2019). Notably, at 5 wt% KOH, the reaction mixture became viscous rather than separating into biodiesel and glycerol phases (Fig. S17 in the supplementary file). Consequently, the upper limit for catalyst loading was set at 4 wt%, and catalyst concentrations beyond this point were not investigated. GC—MS chromatograms and the corresponding analyses at the optimal catalyst loading 2 wt% (Fig. S7 andTable S3) revealed the principal FAME components and their relative abundances. Following the determination of the optimal catalyst loading, the impact of the oil-to-methanol molar ratio on the biodiesel yield was examined.

3.3.2. Oil-to-MeOH molar ratio

The effect of the oil-to-MeOH molar ratio on the biodiesel yield was investigated over the range of 1:3–1:8, while maintaining a KOH-catalyst loading of 2 wt%, a reaction temperature of 40°C, and a reaction time of 60 min (Fig. 5**(b)).** A stoichiometric molar ratio of 1:3 was selected as the baseline. The biodiesel yield increased with increasing oil-to-MeOH ratio, reaching a maximum of 89 % at a 1:6 ratio. This enhancement is attributed to the improved formation of methoxy species on the catalyst surface, which drives the chemical equilibrium in favor of biodiesel production. However, the yield decreased at ratios exceeding 1:6, as excess MeOH negatively impacts biodiesel properties by reducing viscosity, density, and the flash point (Cai et al., 2015; Muhammad et al., 2017). Additionally, glycerol, the reaction byproduct, becomes more soluble in excess MeOH. This increased solubility complicates glycerol separation and shifts the equilibrium back toward the reactants, thereby decreasing the overall yield. GC—MS chromatograms and the corresponding compositional analysis at the optimal 1:6 molar ratio (Fig. S8 **and** Table S4) confirmed the FAME profile of the biodiesel produced.

3.3.3. Reaction temperature

Under fixed conditions of 2 wt% KOH catalyst, a 1:6 oil-to-MeOH molar ratio, and a 60-min reaction time, the temperature was varied from 35°C to 60°C in 5°C intervals **(**Fig. 5**(c)).** The biodiesel yield reached a maximum of 89 % at 40°C but declined significantly to 71 % at 60°C. While, sufficient thermal energy is necessary to overcome mass transfer resistance in a reaction mixture comprising oil, alcohol, and a catalyst, temperatures approaching or exceeding the boiling point of MeOH lead to rapid vaporization and bubble formation, which adversely affect the reaction kinetics. Furthermore, elevated temperatures increase the activation energy for the reverse reaction, thereby hindering biodiesel formation and reducing the final yield (Kawentar and Budiman, 2013). GC—MS chromatograms and the corresponding analysis at 40°C (Fig. S9 **and** Table S5) confirmed the FAME compositions of the biodiesel produced.

3.3.4. Reaction time

Reaction times of 15, 30, 45, 60, 75, and 90 min were evaluated at 15-min intervals, while maintaining a constant KOH catalyst loading (2 wt%), the oil-to-MeOH molar ratio (1:6), and temperature (40°C) **(**Fig. 5**(d)).** The biodiesel yield exhibited a rapid initial increase as the system approached toward equilibrium, however, the yield gradually decreased with further increases in reaction time due to the reverse reaction (Kawentar and Budiman, 2013). The optimal reaction time was identified as 60 min, resulting in a maximum yield of 89 %. GC—MS chromatograms and the corresponding analysis at the 60 min (Fig. S10 **and** Table S6) confirmed the FAME compositions of the biodiesel produced.

3.3.5. Optimization results of the transesterification reaction and 3D plot

The transesterification reaction was conducted to evaluate the feasibility of biodiesel production across several key process parameters: KOH catalyst loading (wt%), the oil-to-MeOH molar ratio, the reaction time (t), and the reaction temperature (T). To determine the optimal

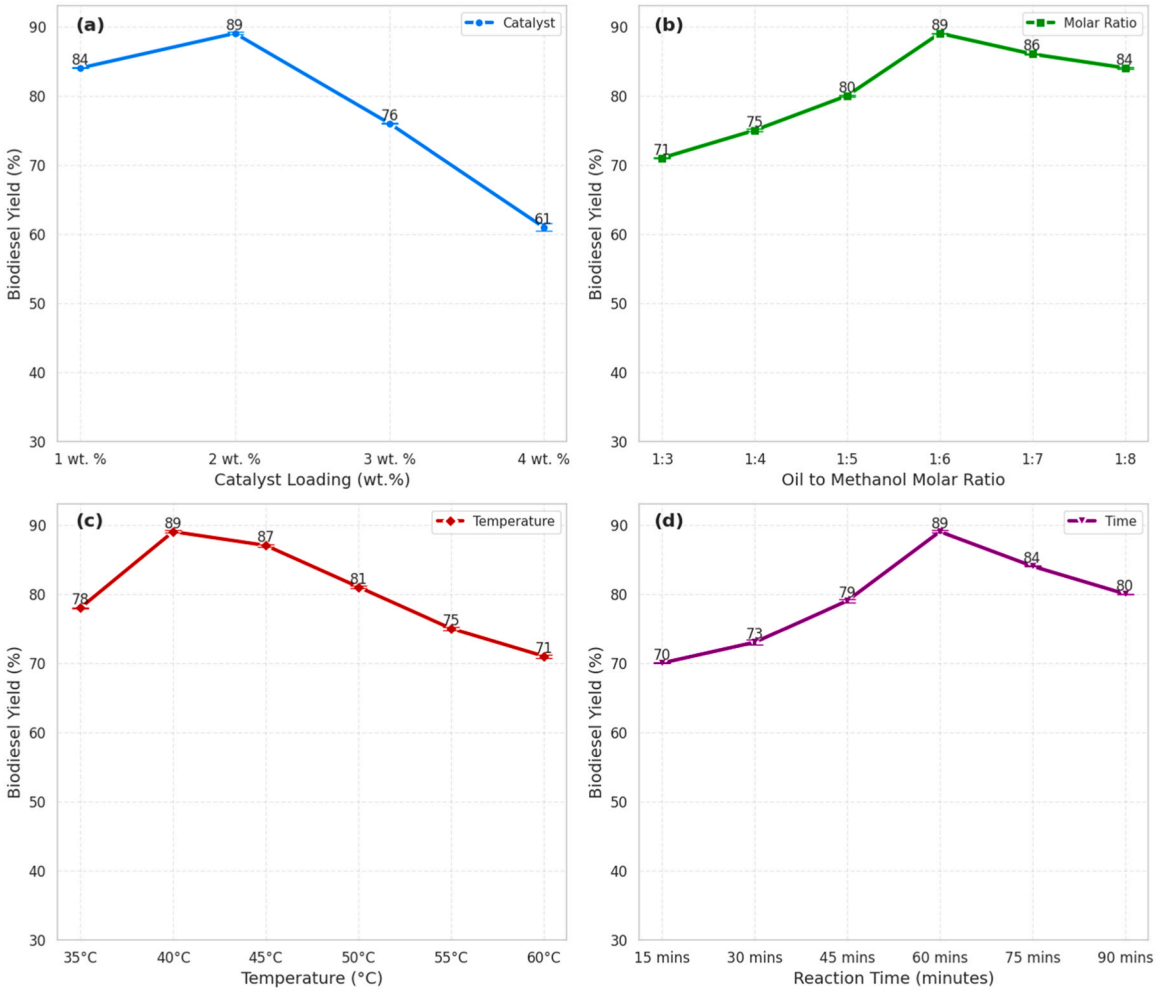


Fig. 5. (a) Impact of catalyst loading (KOH, wt%) on biodiesel yield (%), (b) impact of the oil—to—MeOH molar ratio on biodiesel yield (%), (c) impact of reaction temperature (°C) on biodiesel yield (%), and (d) impact of reaction time (minutes) on biodiesel yield (%). Error bars represent the standard deviation from duplicate experiments, with optimal conditions verification in triplicate.

conditions for each parameter, the experiments were conducted by independently varying the catalyst concentrations (1, 2, 3, 4 and 5 wt %), oil-to-MeOH molar ratios (1:3, 1:4, 1:5, 1:6, 1:7, and 1:8), reaction times (15, 30, 45, 60, 75, and 90 min), and reaction temperatures (35°C, 40°C, 45°C, 50°C, 55°C, and 60°C), while remaining parameters were held constant. All the measurements were conducted in duplicate, with the optimal conditions verified in triplicate to minimize experimental errors. Fig. 6 presents six three-dimensional (3D) surface plots illustrating the effects of dual-parameter interactions on the final biodiesel yield.

The optimal conditions for maximizing the biodiesel yield were consistently identified as a reaction temperature of 40°C, a reaction time of 60 min, a KOH catalyst concentration of 2 wt%, and an oil-to-MeOH molar ratio of 1:6. The response surfaces exhibit parabolic trends, with biodiesel yields peaking within defined parameter ranges and declining beyond these ranges. Specifically, the dual-parameter interactions are illustrated as follows: Fig. 6(a) shows temperature against time; Fig. 6(b) presents temperature versus catalyst concentration; Fig. 6(c) depicts temperature versus the oil-to-MeOH molar ratio; Fig. 6(d) illustrates time and catalyst concentration; Fig. 6(e) shows time against oil-to-MeOH molar ratio; and Fig. 6(f) displays the interaction between catalyst concentration and the oil-to-MeOH molar ratio. Notably, significant interactions were observed between temperature and both the catalyst concentration and the oil-to-MeOH ratio, emphasizing the critical importance of balancing these variables to optimize the reaction efficiency. These findings highlight the necessity of precise parameter optimization to maximize biodiesel yield in transesterification processes. Following the optimization phase, the study subsequently evaluated and compared the performance of the processes, as described in the sections below.

3.4. Process-I: transesterification of esterified oil under optimal conditions without cosolvent

Following the identification of optimal transesterification reaction conditions from the impact assessment and optimization graph (Fig. 5 and Fig. 6), the transesterification of esterified WCO was carried out under optimal conditions—2 wt% KOH catalyst loading, a 1:6 oil-to-methanol molar ratio, 600 rpm agitation, a 60-min reaction time, and a reaction temperature of 40°C without cosolvent. Fig. S11 shows the GC—MS chromatogram of biodiesel synthesized under these optimized conditions. The corresponding GC—MS analysis Table 2 **(A) and** Table S7 revealed the FAME compositions of synthesis biodiesel are as follows: hexadecanoic acid methyl ester (8.47 %, at 36.54 min retention time), 11,14-octadecadienoic acid methyl ester (23.08 %, at 39.84 min), 9-octadecenoic acid (Z) methyl ester (54.37 %, at 40.08 min), methyl stearate (5.16 %, at 40.45 min), and cis-13-eicosenoic acid methyl ester (2.47 %, at 43.47 min). These results align with the published literature on biodiesel from WCO.

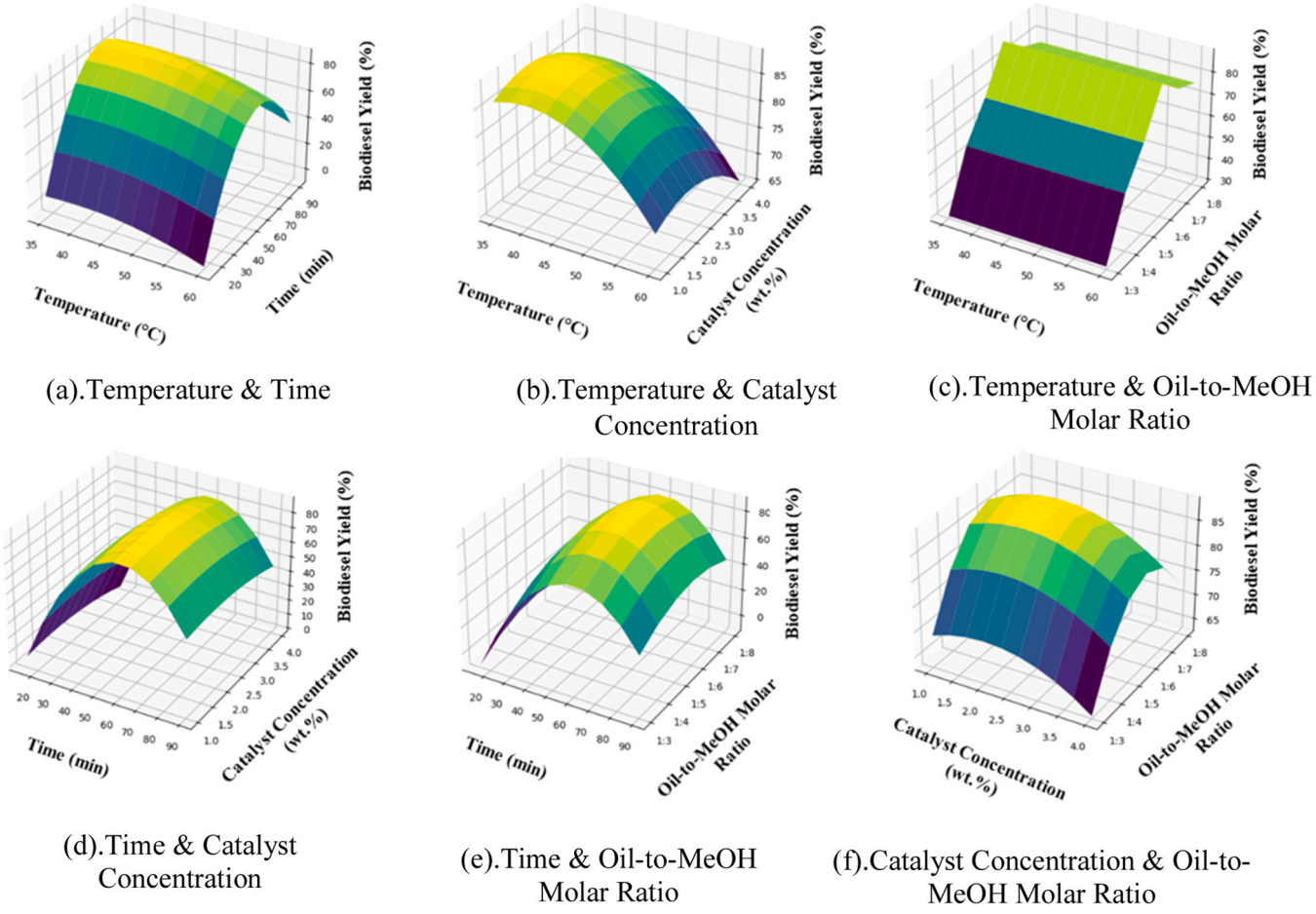


Fig. 6. 3D surface plots versus process conditions: (a) temperature and time, (b) temperature and catalyst concentration, (c) temperature and the oil-to-MeOH molar ratio, (d) time and catalyst concentration, (e) time and the oil-to-MeOH molar ratio, (f) catalyst concentration and the oil-to-MeOH molar ratio, illustrating the interactive effects of process variables on biodiesel yield (%). The 3D plots were generated on the basis of the impact assessment and the optimum values (section 3.3 and corresponding subsection).

3.5. Process-II: transesterification of esterified oil under optimal conditions and 1:6 oil: n-hexane cosolvent

To evaluate the impact of n-hexane on the biodiesel yield, a series of reactions was conducted using oil-to-hexane molar ratios ranging from 1:1–1:6. As shown in Fig. S12, the highest biodiesel yield was achieved at an oil-to-n-hexane cosolvent molar ratio of 1:6. Following this optimization, GC—MS analysis was carried out to confirm the FAME compositions at the optimal ratio. Specifically, Fig. S13 highlights the GC—MS chromatogram and the resulting FAME profile under these transesterification conditions. Furthermore, the corresponding GC—MS data, presented in Table 2 **(B) and** Table S8, provide a detailed composition of the FAME constituents present in the synthesized biodiesel at the optimal oil-to-n-hexane — ratio. For each constituent, the table lists the area percentage in the chromatogram.

Notably, the major FAME components included hexadecanoic acid, methyl ester (9.12 %, at a retention time of 36.54 min), 9-octadecenoic acid (*Z*)-methyl ester (50.12 %, at 40.07 min), and methyl stearate (5.62 %, at 40.45 min). Collectively, this information offers valuable insights into the composition of biodiesel produced under specific cosolvent conditions. The bar chart in Fig. 7 illustrates the impact of the oil-to-n-hexane cosolvent ratio on the biodiesel yield. As the ratio increased from 1:1–1:6, the biodiesel yields significantly improved, reaching a peak value of 96.0 % at a 1:6 ratio. This trend suggests that a higher n-hexane content enhances the efficiency of biodiesel production by improving the miscibility of the oil and methanol phases (Bai et al., 2022). Furthermore, this 1:6 ratio was identified as optimal based on GC—MS analysis, which revealed that a higher percentage of FAMEs corresponded to increased biodiesel yield. Moreover, beyond this ratio, no significant further improvement in yield was observed, reinforcing the use of 1:6 as the ideal cosolvent proportion for maximizing biodiesel output.

3.6. Process-III: transesterification of esterified oil under optimal conditions and 1:6 oil: CPME cosolvent

To evaluate the impact of CPME cosolvent on biodiesel yield, a series of reactions was conducted using oil-to-CPME molar ratios ranging from 1:1–1:7. As shown in Fig. S14, the optimal biodiesel yield was achieved at a 1:6 ratio. Subsequently, GC—MS analysis was performed to verify the FAME compositions at this optimal oil—to—CPME molar ratio. Specifically, Fig. S15 illustrates the FAME profile under the specified transesterification conditions.

Furthermore, the GC—MS data detailed in Table 2 **(C)** and Table S9 provide a comprehensive composition of the FAMEs in the synthesized biodiesel at a 1:6 ratio. Notably, the FAME constituents included hexadecanoic acid, methyl ester (15.57 %, at a retention time of 36.54 min), 11,14-octadecadienoic acid, methyl ester (32.91 %, at 39.87 min), and 9-octadecenoic acid (*Z*)-methyl ester (37.98 %, at 40.04 min).

The bar chart (Fig. 8) illustrates the effect of varying the oil-to-CPME cosolvent ratio on the biodiesel yield. As the ratio increased from 1:1–1:6, the biodiesel yield improved markedly, reaching a maximum of 97.5 % at a 1:6 ratio. This enhancement is attributed to the alleviation of mass transfer resistance between the oil and methanol phases,

Table 2
Comparison of the FAME compositions of synthesized biodiesel (A) without cosolvent, (B) with n-hexane cosolvent, and (C) with CPME cosolvent.

FAME Compositions	Chemical Group	Process-I Without cosolvent (Area%) (A)	Process-II With n-hexane (Area%) (B)	Process-III With CPME (Area%) (C)
Methyl tetradecanoate	Saturated FAME	0.09	0.12	0.23
Methyl hexadeca-9-enoate	Palmitoleic acid (C16:1)	0.77	0.91	0.13
Hexadecanoic acid, methyl ester	Palmitic acid (C16:0)	8.47	9.12	15.57
Cis-10-Heptadecenoic acid, methyl ester	Monounsaturated FAME	-	0.07	0.12
Heptadecanoic acid, methyl ester	Saturated FAME	0.07	0.08	0.20
9-Octadecenoic acid (*Z*)-methyl ester	Oleic acid (C18:1)	54.37	50.12	37.98
9,12,15-Octadecatrienoic acid, methyl ester	Linolenic acid (C18:3)	-	1.59	0.21
Methyl stearate	Stearic acid (C18:0)	5.16	5.62	7.62
Methyl 10-trans, 12-cis-Octadecadienoate	Polyunsaturated FAME	-	0.17	0.20
Methyl (11 R,12 R,13S)-(*Z*)-12,13-epoxy-11-methoxy-9-octadece	Epoxy FAME	-	0.13	0.12
Methyl 18-methylnonadecanoate	Branched-chain FAME	1.62	1.42	0.90
Tetracosanoic acid, methyl ester	Saturated FAME	0.37	0.31	0.26
Methyl 9-cis,11 trans-octadecadienoate	Polyunsaturated FAME	0.35	-	-
Octadec-9-enoic acid	Oleic acid (C18:1)	0.49	-	-
11,14- Octadecadienoic acid, methyl ester	Linoleic acid (C18:2)	23.08	-	32.91
Docosanoic acid, methyl ester	Saturated FAME	-	-	0.78
Cis-11-Eicosenoic acid, methyl ester	Monounsaturated FAME	-	-	0.72
9-Hexadeccenoic acid, methyl ester	Palmitoleic acid (C16:1)	-	-	1.60
17- Octadecynoic acid, methyl ester	Unsaturated FAME	-	-	0.08
7- Octadecenoic acid, methyl ester	Monounsaturated FAME	-	-	0.14
Methyl 9, cis,11,trans.t.13,trans.-octadecatrienoate	Polyunsaturated FAME	-	-	0.23
Cyclopropaneoctanic acid, 2-octyl-, methyl ester, cis-	Cyclopropane FAME	0.17	0.07	-
Cis-11,14-Ecosadienoic acid, methyl ester	Polyunsaturated FAME	0.13	0.12	-
Cis-13-Eicosenoic acid, methyl ester	Monounsaturated FAME	2.47	2.29	-
Methyl 20-methyl-heneicosanoate	Branched-chain FAME	0.79	0.74	-
15-Tetracosenoic acid, methyl ester, (*Z*)-	Monounsaturated FAME	0.19	0.15	-
9,12, Octadecadienoic acid (ZZ), methyl ester	Linoleic acid (C18:2)	-	22.02	-
9-octadecenoic acid, methyl ester (E)	Oleic acid (C18:1)	-	5.17	-
6-octadecenoic acid, methy ester (Z)$^{-}$	Monounsaturated FAME	-	0.14	-

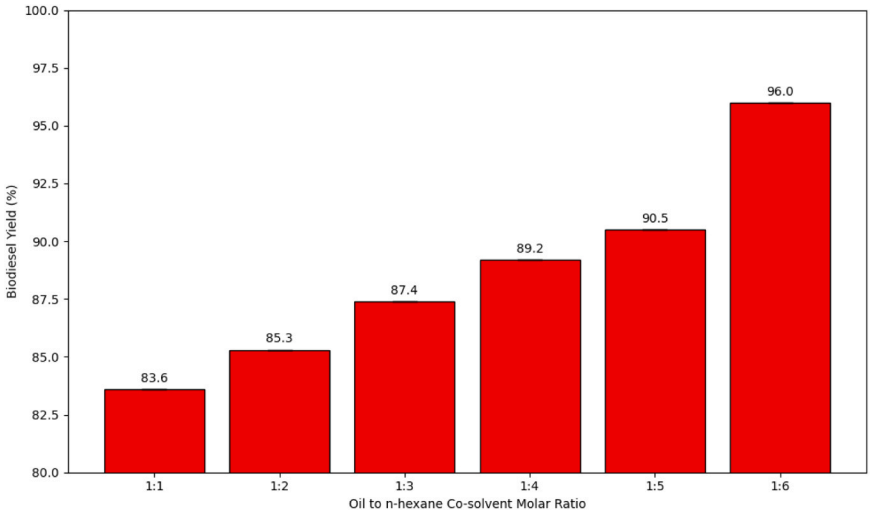


Fig. 7. Impact of the n-hexane cosolvent molar ratio on the biodiesel yield (%). Error bars represent the standard deviation from duplicate experiments, with optimal conditions verification in triplicate.

facilitating a more homogenous reaction environment. Beyond this optimal ratio, the yield plateaued, with no statistically significant improvement observed. GC—MS analysis conducted at a 1:7 ratio in Fig. S16 **and** Table S10 confirmed that the FAME content remained comparable to the 1:6 ratio, indicating no further increase in biodiesel yield. However, increasing the cosolvent ratio beyond 1:7 introduces difficulties in separating biodiesel and glycerol phases, which is attributed to the dilution effects caused by excessive cosolvent addition. A similar trend was observed for n-hexane, where the biodiesel yield did not improve beyond the optimal cosolvent ratio. This phenomenon is consistent with findings from studies involving other cosolvents (Ambat et al., 2020; Bai et al., 2022; Miyuranga et al., 2022; Felicia, 2014). Consequently, the 1:6 oil-to-CPME molar ratio was identified as optimal, which is supported by the GC—MS results showing the highest FAME percentage at this point. Notably, it is noteworthy that despite thorough purification, the biodiesel synthesized using both n-hexane and CPME cosolvents retained residual odors characteristic of the respective cosolvents.

3.7. Impact of cosolvents on FAME compositions

The data in Table 2 reveal significant differences in the area

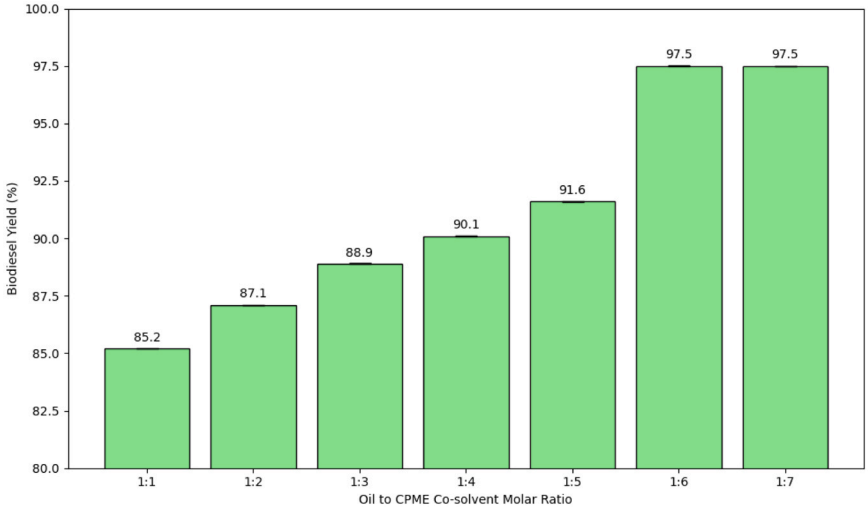


Fig. 8. Impact of the CPME cosolvent molar ratio on the biodiesel yield (%). Error bars represent the standard deviation from duplicate experiments, with optimal conditions verification in triplicate.

percentages of specific FAMEs, particularly 9-octadecenoic acid (*Z*)-methyl ester and hexadecenoic acid methyl ester, illustrating how cosolvents can distinctly influence the composition of biodiesel. The effectiveness of a cosolvent in transesterification reaction depends on its dielectric constant, dipole moment, polarity, polarity index, and its capacity to dissolve reactants. CPME and n-hexane differ markedly in terms of their physical and chemical properties. Specifically, the CPME results in higher values for the dielectric constant (4.76), dipole moment (1.27), and polarity index (2.8), alongside a higher boiling point (106°C), flash point (-12°C), and density (0.86 g/cm^3), than those of n-hexane in Table S11.

Notably, CPME possesses intermediate polarity, whereas n-hexane is nonpolar. These differences in polarity and physicochemical properties enable CPME cosolvents to alter the reaction environment and potentially stabilize intermediates or transition states in various ways. This can lead to variations in the reaction rate and the conversion efficiency. The fundamental rationale for CPME's enhanced performance lies in its intermediate polarity, which creates a homogenous phase between the polar methanol and the nonpolar oil, effectively eliminating mass transfer barriers. This is quantified by its dielectric constant (4.76) and polarity index (2.8), positioning it between methanol (32.6) and triglyceride oil (~3), which enables the effective solubilization of both reactants. In contrast, the nonpolar nature of n-hexane ($\varepsilon = 1.9$) makes it a less effective cosolvent for solubilizing the polar methanol, resulting in slightly lower miscibility and consequently, a lower yield. Furthermore, CPME's higher boiling point (106°C) offers a safer operational window compared to the highly volatile n-hexane (BP 69°C).

Additionally, the superior performance of CPME is supported by a range of experimental evidence: the postreaction mixture with CPME (Fig. 2f) showed a substantially smaller glycerol phase than the no-cosolvent (Fig. 2d) or n-hexane (Fig. 2e) systems, indicating more complete conversion. This visual evidence correlates with distinct FAME composition changes in CPME-derived biodiesel (Table 2), notably a significant increase in methyl palmitate (15.57 %) and a pronounced shift toward 11,14- Octadecadienoic acid, methyl ester (32.91 %). These compositional differences suggest CPME's intermediate polarity creates a unique reaction environment that influences FAME distribution. Collectively, the reduced glycerol volume, altered FAME profile, and highest achieved yield (97.5 % provide consistent evidence that CPME enhances reactant miscibility during transesterification, thereby reducing mass transfer limitation and improving overall conversion efficiency.

Furthermore, the data show that the percentage area of 9-octadecenoic acid (*Z*)-methyl ester (oleic acid methyl ester) decreases markedly in the presence of CPME relative to both the no-cosolvent and n-hexane conditions. These findings suggest that CPME may specifically interact with oleic acid methyl ester, promoting its enhanced conversion into other FAMEs. Conversely, the area percentages of hexadecanoic acid and methyl ester (palmitic acid methyl ester) increased significantly with CPME compared with both n-hexane and no-cosolvent, indicating that CPME more effectively facilitates the formation or stabilization of this specific ester. These findings highlight that different cosolvents can influence the selectivity of the transesterification reaction toward particular FAMEs. However, compared with n-hexane, and without cosolvent, CPME favors the production of hexadecanoic acid, methyl ester, 11,14-octadecadienoic acid, and methyl ester. CPME, with its moderate polarity, likely creates a more favorable reaction medium for the synthesis and stabilization of certain FAMEs, thereby improving overall yields and altering product distribution. In contrast, the nonpolar nature of n-hexane may limit its ability to solubilize key intermediates effectively, resulting in slightly lower yields and different FAME profiles than those of CPME.

Moreover, the highest percentage of 9-octadecenoic acid (*Z*)-methyl ester observed without cosolvent decreased significantly with the addition of either n-hexane or CPME. This behavior could be attributed to differences in solubility or possible stabilization effects on intermediates within the reaction system. These observations regarding the effects of cosolvent on biodiesel composition are consistent with reports in the literature (Singh et al., 2017; Encinar et al., 2016; Okitsu et al., 2013; Mohadesi et al., 2020; Díaz et al., 2023).

3.8. Comparative biodiesel yield (%) analysis

The bar chart in Fig. 9 compares the biodiesel yield percentages under three different conditions: without a cosolvent, with an n-hexane cosolvent, and with a CPME cosolvent. The biodiesel yield without a cosolvent reached 89 %, which increased to 96 % with n-hexane and further to 97.5 % with CPME at the optimal 1:6 oil-to-cosolvent molar ratio. While the 1.5 % absolute yield increase with CPME is valuable, its practical significance must be assessed against the process economics of solvent recovery. A simplified comparative energy analysis, based on the latent heat of vaporization, was performed to contextualize this yield gain. The energy required to recover CPME (BP 106°C) was estimated to be approximately 15.6 % higher per mole than n-hexane (BP 68.7°C) (Appendix- XIII). Thus, the marginal yield benefit of CPME must be balanced against the higher operational energy costs for its recovery in

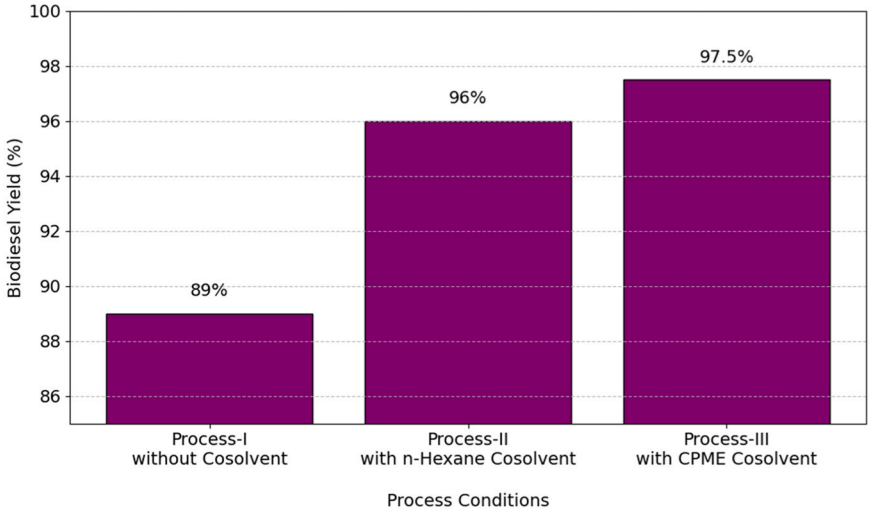


Fig. 9. The biodiesel yield (%) under different process conditions: (1) without cosolvents, (2) with n-hexane cosolvent, and (3) with CPME cosolvent.

an industrial setting.

Despite this energy trade-off, CPME offers significant advantages in terms of process safety, as it has a higher flash point (-1°C) and lower toxicity compared to n-hexane (flash point = −22°C), which is a widely available petrochemical solvent. Furthermore, CPME's potential for bio-based production provides a more viable sourcing pathway compared to petroleum-derived n-hexane.

Table 2 presents the detailed FAME composition of the synthesized biodiesel under three different conditions. A progressive increase in biodiesel yield was observed across oil-to-cosolvent ratios from 1:4–1:6 for both n-hexane and CPME, as illustrated in Fig. 7 & Fig. 8. Conversely, at lower cosolvent ratios (1:1–1:3), the addition of cosolvents has a noticeably negative effect on the biodiesel yield compared to the baseline (89 % biodiesel yield), as shown in Fig. 9.

Two potential factors may explain this reduced yield at suboptimal cosolvent ratios. First, the transesterification process, which consists of three consecutive and reversible reactions converting triglycerides to diglycerides, then monoglycerides, and finally glycerol and FAME-, may not have been effectively facilitated by the cosolvents at these lower ratios. Insufficient cosolvent levels likely lead to incomplete homogenization of the methanol and oil phases, limiting the formation rates of mono and diglyceride intermediates, thereby reducing reaction efficiency. Second, the polarity and relatively low kinematic viscosity of the cosolvents at these ratios may have contributed to the reduced catalytic activity. These explanations are consistent with observations reported in the literature (İlgen et al., 2009; Putra et al., 2015; Sahani et al., 2018).

Collectively, these findings indicate that the addition of a cosolvent enhances the transesterification process only when it was employed in optimal quantities by improving the miscibility between the oil and MeOH phases. Consequently, cosolvent usage below the optimal ratio adversely affects biodiesel yield, whereas excessive cosolvent addition complicates phase separation and purification. The significant enhancement in yield from the optimized baseline (89 %) to the cosolvent-assisted processes (96 % and 97.5 %) clearly validates the cosolvent's role as an effective reaction intensifier under optimal conventional conditions, confirming a successful mitigation of mass transfer limitations. Therefore, determining the optimal oil-to-cosolvent ratio specific to each reaction system is critical for maximizing performance. Furthermore, a comparative analysis between n-hexane and CPME reveals that CPME consistently yields higher biodiesel outputs across all tested ratios. For example, at a 1:6 ratio, CPME achieves a yield of 97.5 %, surpassing the 96 % yield obtained with n-hexane. This superior performance can be attributed to the favorable chemical properties of CPME, including enhanced polarity, lower volatility, and potentially reduced tendency to form byproducts during transesterification.

Moreover, the core biodiesel quality parameter, the FAME content was determined to be 99.87 % for n-hexane and 99.88 % for the CPME, both of which exceed the minimum requirement of 96.5 % established by the European Union EN 14214 biodiesel quality standard. This demonstrates full compliance with the EN 14214 specification. Furthermore, the FAME compositions of the synthesized biodiesel were found to be consistent with those reported in the literature (Xia et al., 2024; Mohammad et al., 2013). Additionally, Table 3 presents a comparative analysis of this study alongside other investigations on biodiesel production from WCO, encompassing various cosolvents, catalysts, reactor types, and reaction conditions. This table highlights the

Table 3
Comparison of this study with other cosolvent studies.

Cosolvent	Catalyst	Reactor type	Feedstock	Reaction conditions						Yield (wt%)	Ref.
				Oil: Cosolvent ratio/amount	Catalyst amount (wt %)	Oil: MeOH/ molar ratio	Time (min)	T (∘C)	Stir (rpm)		
n-hexane (Ultrasound-assisted)	KOH	Three- neck batch	WCO	1:8	2	1:6	20	40	-	98.5	(Bai et al., 2022)
n-hexane	CaO	Micro reactor	WCO	58 vol%	8.17	51.3 vol%	10	62	-	97.02	(Aghel et al., 2018)
n-hexane	KOH	Erlenmeyer flask	WCO	1:6	2	1:6	60	40	600	96	This study
CPME	KOH	Erlenmeyer flask	WCO	1:6	2	1:6	60	40	600	97.5	

biodiesel yield percentages achieved under each set of conditions, thereby illustrating the relative efficiency of different methodologies in converting WCO to biodiesel.

3.9. Possible limitations of this study

It is critical to note that the environmental benefits of using CPME are contingent upon its efficient recovery and reuse, which was not implemented in the laboratory-scale study. Venting solvents to the atmosphere is not a sustainable practice; therefore, the future scalability and true 'green' credentials of this process depend on integrating a solvent recovery unit, such as vacuum distillation, and demonstrating its effective recycling over multiple batches. Additionally, the cosolvent comparison, using a pragmatic, hierarchical approach, clearly measured the performance boost under optimized baseline conditions. However, full, independent optimization of all four process variables was not conducted to find the absolute maximum yield for each system.

4. Conclusions and future outlooks

This research investigated a two-step process for biodiesel production from WCO via acidic esterification followed by homogeneous base-catalyzed transesterification. Using an experimental trial-and-error optimization approach, the optimal esterification conditions- 5 wt% H_2SO_4 catalyst, a 1:10 oil-to-methanol molar ratio, 60°C temperature, and a 120-min reaction time- effectively reduced the FFA content in WCO from 10.7 % to 0.89 %, enabling efficient base-catalyzed transesterification. The optimal baseline transesterification conditions - 2 wt % KOH catalyst, a 1:6 oil-to-MeOH molar ratio, 40°C reaction temperature, and a 60-min reaction time- yielded 89 % biodiesel yield without a cosolvent. Further investigation and GC—MS analysis confirmed that incorporating a cosolvent, specifically either low-toxicity CPME or n-hexane (at an optimal 1:6 oil-to-cosolvent molar ratio), to the alkaline transesterification process significantly enhanced the performance of the optimized baseline process. The yield increased from 89 % to 97.5 % with CPME and 96 % with n-hexane, both meeting the European Union EN 14214 biodiesel quality standard (≥96.5 % FAME). CPME outperformed n-hexane by improving miscibility between the oil and methanol phases, thereby enhancing mass transfer and reducing interfacial resistance. Furthermore, compared with other alternative solvent systems, such as supercritical CO_2 (86.33 %) and deep eutectic solvents (≈ 44 %), CPME demonstrated superior conversion efficiency and more favorable handling properties. Additionally, the use of cosolvent facilitated operation at reduced process temperature, potentially contributing to lower energy requirements.

In this study, unreacted MeOH and n-hexane were removed via rotary evaporation, while CPME was evaporated under a fume hood. It is important to note that venting solvents represents a limitation for process sustainability, so future work must integrate closed-loop recovery systems. Subsequently research should focus on kinetic viscosity studies at varying CPME ratios, mechanistic elucidation via nuclear magnetic resonance (NMR), and density functional theory (DFT) simulations, and the optimization of the oil-to-cosolvent ratio for diverse WCO qualities to ensure the process's broad applicability and reliability across varying feedstocks. These approaches will provide deeper insights into reaction effectiveness and feedstock versatility. Finally, comprehensive techno-economic analyses are also recommended to evaluate energy demands and cost-effectiveness, particularly concerning solvent recovery under vacuum distillation, to support the transition of this process toward industrial-scale biodiesel production.

CRediT authorship contribution statement

Md. Rubel: Conceptualization, Methodology, Writing – original draft, Visualization, Validation, Formal analysis, Data curation. **Cheng Shuo:** Co-supervision, Writing – review & editing, Validation, Investigation, Resource. **Sasipa Boonyubol:** Writing – review & editing, Validation, Investigation. **M.M. Harussani:** Writing – review & editing. **Surendra Singh Kachhwaha:** Writing – review & editing, Validation and Investigation. **Jeffrey S. Cross:** Supervision, Conceptualization, Methodology, Writing – review & editing, Validation, Investigation, Resources, Project administration, Funding acquisition.

Consent to publish

All authors have reviewed and approved the manuscript's content and granted explicit permission for its publication.

Declaration of Generative AI and AI-assisted technologies in the writing process

During the preparation of this work, the author (s) used ChatGPT Plus, Quill Bot, and Grammarly to paraphrase and edit the language while ensuring that all research findings and interpretations remained original. Additionally, after using these tools, the author(s) carefully reviewed and edited the content as needed and take (s) full responsibility for the content of the published article.

Funding

This work was supported by the Ministry of Education, Culture, Sports, Science and Technology (MEXT), Japan, through the Japanese Government Scholarship program awarded to the first author. There is no specific grant ID associated with this scholarship.

Declaration of Competing Interest

The author declares no known financial conflicts of interest or personal relationships that could have influenced the work reported in this study.

Acknowledgments

The author thanks the local restaurant authority in Tokyo for their invaluable support and cooperation in facilitating the collection of samples for this study. The first author acknowledges the financial support provided by the Japan Ministry of Education, Culture, Sports, Science and Technology (MEXT) through the MEXT scholarship for graduate studies. The author also thanks Professor Koichi Mikami and Eric Kolor, along with other students in the Cross Lab at Science Tokyo, for their guidance and suggestions in writing this manuscript.

Appendix A. Supporting information

Supplementary data associated with this article can be found in the online version at doi:10.1016/j.cherd.2026.01.005.

Data Availability

The data supporting the findings of this study are available in the supplementary data file. Further explanation can be provided upon request.

References

A Zayed, M., SM Abd El-Kareem, M., Zaky, N., 2016. Gas chromatography-mass spectrometry studies of waste vegetable mixed and pure used oils and its biodiesel products. J. Pharm. Appl. Chem. 2, 30–37.

Abidin, S.Z., Haigh, K.F., Saha, B., 2012. Esterification of free fatty acids in used cooking oil using ion-exchange resins as catalysts: an efficient pretreatment method for biodiesel feedstock. Ind. Eng. Chem. Res. 51, 14653–14664.

Abrante-Pascual, S., Nieva-Echevarría, B., Goicoechea-Oses, E., 2024. Vegetable oils and their use for frying: a review of their compositional differences and degradation. Foods 13, 4186.

Aghel, B., Mohadesi, M., Sahraei, S., 2018. Effect of different cosolvents on transesterification of waste cooking oil in a microreactor. Chem. Eng. Technol. 41, 598–605.
Al-Saadi, A., Mathan, B., He, Y., 2020. Biodiesel production via simultaneous transesterification and esterification reactions over SrO–ZnO/Al2O3 as a bifunctional catalyst using high acidic waste cooking oil. Chem. Eng. Res. Des. 162, 238–248.
Alias, N.I., Jayakumar, J., Zain, S.M., 2018. Characterization of waste cooking oil for biodiesel production. J. Kejuruter. 1, 79–83.
Ali, L., Fadhil, A., 2013. Biodiesel production from spent frying oil of fish via alkali-catalyzed transesterification. Energy Sources Part A Recovery Util. Environ. Eff. 35, 564–573.
Altikriti, E., Fadhil, A., Dheyab, M., 2015. Two-step base catalyzed transesterification of chicken fat: optimization of parameters. Energy Sources Part A Recovery Util. Environ. Eff. 37, 1861–1866.
Ambat, I., Srivastava, V., Iftekhar, S., Haapaniemi, E., Sillanpää, M., 2020. Effect of different co-solvents on biodiesel production from various low-cost feedstocks using Sr–Al double oxides. Renew. Energy 146, 2158–2169.
Bai, H., Tian, J., Talifu, D., Okitsu, K., Abulizi, A., 2022. Process optimization of esterification for deacidification in waste cooking oil: RSM approach and for biodiesel production assisted with ultrasonic and solvent. Fuel 318, 123697.
Bart, J.C., Palmeri, N., Cavallaro, S., 2010. Biodiesel Science Technology Soil Oil. Elsevier.
Baskar, G., Selvakumari, I.A.E., Aiswarya, R., 2018. Biodiesel production from castor oil using heterogeneous Ni doped ZnO nanocatalyst. Bioresour. Technol. 250, 793–798.
Bhatia, S.K., Bhatia, R.K., Jeon, J.-M., Pugazhendhi, A., Awasthi, M.K., Kumar, D., et al., 2021. An overview on advancements in biobased transesterification methods for biodiesel production: oil resources, extraction, biocatalysts, and process intensification technologies. Fuel 285, 119117.
Cai, Z.-Z., Wang, Y., Teng, Y.-L., Chong, K.-M., Wang, J.-W., Zhang, J.-W., et al., 2015. A two-step biodiesel production process from waste cooking oil via recycling crude glycerol esterification catalyzed by alkali catalyst. Fuel Process. Technol. 137, 186–193.
Cerón Ferrusca, M., Romero, R., Martínez, S.L., Ramírez-Serrano, A., Natividad, R., 2023. Biodiesel production from waste cooking oil: a perspective on catalytic processes. Processes 11, 1952.
Chilakamarry, C.R., Sakinah, A.M., Zularisam, A., Pandey, A., 2021. Glycerol waste to value added products and its potential applications. Syst. Microbiol. Biomanuf. 1, 378–396.
Degfie, T.A., Mamo, T.T., Mekonnen, Y.S., 2019. Optimized biodiesel production from waste cooking oil (WCO) using calcium oxide (CaO) nano-catalyst. Sci. Rep. 9, 18982.
Díaz, L., Horstmann, F., Brito, A., González, L., 2023. A comprehensive review of the influence of co-solvents on the catalysed methanolysis process to obtain biodiesel. Heliyon 9.
Emmanouilidou, E., Lazaridou, A., Mitkidou, S., Kokkinos, N.C., 2024. A comparative study on biodiesel production from edible and non-edible biomasses. J. Mol. Struct. 1306, 137870.
Encinar, J.M., Pardal, A., Sánchez, N., 2016. An improvement to the transesterification process by the use of co-solvents to produce biodiesel. Fuel 166, 51–58.
ExxonMobil. ExxonMobil. (2024). Energy demand: Three drivers. ExxonMobil. ⟨https://corporate.exxonmobil.com/what-we-do/energy-supply/global-outlook/energy-demand⟩. ExxonMobil.; 2024.
Fadhil, A.B., Saleh, L.A., Altamer, D.H., 2020. Production of biodiesel from non-edible oil, wild mustard (Brassica juncea L.) seed oil through cleaner routes. Energy Sources Part A Recovery Util. Environ. Eff. 42, 1831–1843.
Felicia, F., 2014. Biodiesel Production from Chicken Fat Using 1, 38–42.
Girish, N., Niju, S.P., Begum, K.M.M.S., Anantharaman, N., 2013. Utilization of a cost effective solid catalyst derived from natural white bivalve clam shell for transesterification of waste frying oil. Fuel 111, 653–658.
de Gonzalo, G., Alcántara, A.R., Domínguez de María, P., 2019. Cyclopentyl methyl ether (CPME): a versatile eco-friendly solvent for applications in biotechnology and biorefineries. ChemSusChem 12, 2083–2097.
Gouran, A., Aghel, B., Nasirmanesh, F., 2021. Biodiesel production from waste cooking oil using wheat bran ash as a sustainable biomass. Fuel 295, 120542.
Grosmann, M.T., Andrade, T.A., di, Bitonto, L., Pastore, C., Corazza, M.L., Tronci, S., et al., 2022. Hydrated metal salt pretreatment and alkali catalyzed reactive distillation: a two-step production of waste cooking oil biodiesel. Chem. Eng. Process. Process. Intensif. 176, 108980.
Guo, M., Jiang, W., Chen, C., Qu, S., Lu, J., Yi, W., et al., 2021. Process optimization of biodiesel production from waste cooking oil by esterification of free fatty acids using La3+/ZnO-TiO2 photocatalyst. Energy Convers. Manag. 229, 113745.
Haq, I. ul, Akram, A., Nawaz, A., Abbas, S.Z., Xu, Y., Rafatullah, M., 2021. Comparative analysis of various waste cooking oils for esterification and transesterification processes to produce biodiesel. Green. Chem. Lett. Rev. 14, 462–473.
Hassan, M.M., Fadhil, A.B., 2025. Development of an effective solid base catalyst from potassium based chicken bone (K-CBs) composite for biodiesel production from a mixture of non-edible feedstocks. Energy Sources Part A Recovery Util. Environ. Eff. 47, 8056–8071.
İlgen, O., Akin, A.N., Boz, N., 2009. Investigation of biodiesel production from canola oil using Amberlyst-26 as a catalyst. Turk. J. Chem. 33, 289–294.
India's WCO. Diesel doped with biodiesel made from used cooking oil rolled out. Economic Times. ⟨https://energy.economictimes.indiatimes.com/news/oil-and-gas/diesel-doped-with-biodiesel-made-from-used-cooking-oil-rolled-out/82398223⟩; 2023.
De Jesus, S.S., Ferreira, G.F., Moreira, L.S., Filho, Maciel, 2020. R. Biodiesel production from microalgae by direct transesterification using green solvents. Renew. Energy 160, 1283–1294.
Jin, C., Zhang, X., Han, W., Geng, Z., Thomas, M.T.M., Jeffrey, A.D., et al., 2020. Macro and micro solubility between low-carbon alcohols and rapeseed oil using different co-solvents. Fuel 270, 117511.
Joorasty, M., Rahbar-Kelishami, A., Hemmati, A., 2022. A performance comparison of cyclopentyl methyl ether (CPME) and hexane solvents in oil extraction from sewage sludge for biodiesel production; RSM optimization. J. Mol. Liq. 368, 120573.
Julianto, T., Nurlestari, R., 2018. The Effect of Acetone Amount Ratio as Co-solvent to Methanol in Transesterification Reaction of Waste Cooking Oil, 349. IOP Publishing, 012063.
Kanna, R., 2018. Biodiesel production from waste cooking oil using co-solvent technique. Int. J. Res Appl. Sci. Eng. Technol. 6, 1573–1574.
Kawentar, W.A., Budiman, A., 2013. Synthesis of biodiesel from second-used cooking oil. Energy Procedia 32, 190–199.
Khan, H.M., Iqbal, T., Ali, C.H., Javaid, A., Cheema, I.I., 2020. Sustainable biodiesel production from waste cooking oil utilizing waste ostrich (Struthio camelus) bones derived heterogeneous catalyst. Fuel 277, 118091.
Kumar, S., Shamsuddin, M.R., Farabi, M.A., Saiman, M.I., Zainal, Z., Taufiq-Yap, Y.H., 2020. Production of methyl esters from waste cooking oil and chicken fat oil via simultaneous esterification and transesterification using acid catalyst. Energy Convers. Manag. 226, 113366.
Lamatinulu, L., 2022. The Effect of n-hexane as co-solvent in direct trans esterification of spirulina plantensis using microwave. World J. Adv. Res. Rev. 16, 741–746.
Liu, S., Li, Z., Han, K., Wang, Y., Niu, S., Liu, J., et al., 2024. Biodiesel production from waste cooking oil through transesterification catalyzed by the strontium-zinc bifunctional oxides. Chem. Eng. Process. Process. Intensif. 200, 109777.
Maddikeri, G.L., Pandit, A.B., Gogate, P.R., 2012. Intensification approaches for biodiesel synthesis from waste cooking oil: a review. Ind. Eng. Chem. Res. 51, 14610–14628.
Manzoor, S., Masoodi, F., Rashid, R., Ahmad, M., ul, Kousar, M., 2022. Quality assessment and degradative changes of deep-fried oils in street fried food chain of Kashmir, India. Food Control 141, 109184.
Mariana, R., Susanti, E., Hidayati, L., 2020. The analysis of protein, fat and free fatty acid content changes in fried chicken cooked with repeated cooking oil at street vendors in Malang. IOP Publ. 462, 012019.
Ma, F., Clements, L.D., Hanna, M.A., 1998. Biodiesel fuel from animal fat. Ancillary studies on transesterification of beef tallow. Ind. Eng. Chem. Res. 37, 3768–3771.
Mićić, R., Tomić, M., Martinović, F., Kiss, F., Simikić, M., Aleksic, A., 2019. Reduction of free fatty acids in waste oil for biodiesel production by glycerolysis: investigation and optimization of process parameters. Green. Process. Synth. 8, 15–23.
Midha, A., Tomar, A., 2023. Towards Achieving Net Zero Emissions in India by 2070. Springer, pp. 981–991.
Ministry of Economy, Trade and Industry, Japan. (2015). Japan's energy plan. Ministry of Economy, Trade and Industry. ⟨https://www.meti.go.jp/english/press/2015/1012_01.html⟩. Ministry of Economy, Trade and Industry, Japan.; 2015.
Miyuranga, K.V., Arachchige, U.S., Marso, T., Samarakoon, G., 2023. Biodiesel production through the transesterification of waste cooking oil over typical heterogeneous base or acid catalysts. Catalysts 13, 546.
Miyuranga, K.V., Balasuriya, B., Arachchige, U., Thilakarathne, D., Jayasinghe, R., Weerasekara, N., 2022. Production of biodiesel using acetone as a co-solvent. Int. J. Eng. Sci. 6, 52–56.
Mohadesi, M., Aghel, B., Gouran, A., Razmehgir, M.H., 2022. Transesterification of waste cooking oil using Clay/CaO as a solid base catalyst. Energy 242, 122536.
Mohadesi, M., Aghel, B., Maleki, M., Ansari, A., 2020. Study of the transesterification of waste cooking oil for the production of biodiesel in a microreactor pilot: the effect of acetone as the co-solvent. Fuel 273, 117736.
Mohammad, M., Hari, T.K., Yaakob, Z., Sharma, Y.C., Sopian, K., 2013. Overview on the production of paraffin based-biofuels via catalytic hydrodeoxygenation. Renew. Sustain. Energy Rev. 22, 121–132.
Moklis, M.H., Cheng, S., Cross, J.S., 2023. Current and future trends for crude glycerol upgrading to high value-added products. Sustainability 15, 2979.
Moklis, M.H., Shuo, C., Boonyubol, S., Cross, J.S., 2024. Electrochemical valorization of glycerol via electrocatalytic reduction into biofuels: a review. ChemSusChem 17, e202300990.
Muhammad, A.B., Obianke, M., Gusau, L.H., Aliero, A.A., 2017. Optimization of process variables in acid catalysed in situ transesterification of Hevea brasiliensis (rubber tree) seed oil into biodiesel. Biofuels 8, 585–594.
Muppaneni, T., Reddy, H.K., Deng, S., 2015. Supercritical synthesis of ethyl esters via transesterification from waste cooking oil using a co-solvent. J. Environ. Prot. 6, 986.
Najaf-Abadi, M.K., Ghobadian, B., Dehghani-Soufi, M., 2024. A review on application of deep eutectic solvents as green catalysts and co-solvents in biodiesel production and purification processes. Biomass. Convers. Biorefinery 14, 3117–3134.
Okitsu, K., Sadanaga, Y., Takenaka, N., Maeda, Y., Bandow, H., 2013. A new co-solvent method for the green production of biodiesel fuel–optimization and practical application. Fuel 103, 742–748.
Pace, V., Hoyos, P., Castoldi, L., Domínguez de María, P., Alcántara, A.R., 2012. 2-Methyltetrahydrofuran (2-MeTHF): a biomass-derived solvent with broad application in organic chemistry. ChemSusChem 5, 1369–1379.
Parija, P., 2022. India's Dependence on Imported Cooking Oil to Continue. Al Jazeera. ⟨https://www.aljazeera.com/economy/2022/1/24/indias-dependence-on-imported-cooking-oil-to-continue⟩.
Paryanto, I., Prakoso, T., Suyono, E.A., Gozan, M., 2019. Determination of the upper limit of monoglyceride content in biodiesel for B30 implementation based on the measurement of the precipitate in a Biodiesel–Petrodiesel fuel blend (BXX). Fuel 258, 116104.

Di Pietro, M.E., Mannu, A., Mele, A., 2020. NMR determination of free fatty acids in vegetable oils. Processes 8, 410.
Prajapati, N., Kachhwaha, S.S., Kodgire, P., Vij, R.K., 2024. Analysis of a novel high-speed homogenizer technique for methyl ester production using waste cooking oil: multi-objective optimization and energy analysis. Chem. Eng. Res. Des. 203, 478–491.
Putra, R.S., Hartono, P., Julianto, T.S., 2015. Conversion of methyl ester from used cooking oil: the combined use of electrolysis process and chitosan. Energy Procedia 65, 309–316.
Rahma, F.N., Hidayat, A., 2023. Biodiesel production from free fatty acid using ZrO (2)/bagasse fly ash catalyst. Int. J. Technol. 14, 206–218.
Sadaf, S., Iqbal, J., Ullah, I., Bhatti, H.N., Nouren, S., Nisar, J., et al., 2018. Biodiesel production from waste cooking oil: an efficient technique to convert waste into biodiesel. Sustain. Cities Soc. 41, 220–226.
Sahani, S., Banerjee, S., Sharma, Y.C., 2018. Study of˙co-solvent effect˙on production of biodiesel from Schleichera oleosa oil using a mixed metal oxide as a potential catalyst. J. Taiwan Inst. Chem. Eng. 86, 42–56.
Sakamoto, S., 2013. Contribution of cyclopentyl methyl ether (CPME) to green chemistry. Chim. Oggi-Chem. Today 31, 24–27.
Salleh, W., Muhamat, W., Nurulain, S., Salim, M., Manap, H., 2023. A spectroscopy study of heated palm cooking oil using an open path optical method for Free Fatty Acids concentration measurement. Mater. Today. Proc.
Simonelli, G., Júnior, J.M.F., de Moraes Pires, C.A., dos Santos, L.C.L., 2020. Biodiesel production using co-solvents: a review. Res. Soc. Dev. 9 e99911672–e99911672.
Singh, V., Yadav, M., Sharma, Y.C., 2017. Effect of co-solvent on biodiesel production using calcium aluminium oxide as a reusable catalyst and waste vegetable oil. Fuel 203, 360–369.
Smith, E.L., Abbott, A.P., Ryder, K.S., 2014. Deep eutectic solvents (DESs) and their applications. Chem. Rev. 114, 11060–11082.
Statista Inc. (2023). Food self-sufficiency ratio of oils and fats in Japan. Statista. ⟨https://www.statista.com/statistics/1040066/japan-food-self-sufficiency-ratio-oils-fats/⟩. Statista Inc.; 2023.
Taher, H., Al-Zuhair, S., 2017. The use of alternative solvents in enzymatic biodiesel production: a review. Biofuels Bioprod. Bioref. 11, 168–194.
The Asahi Shimbun Company. (2024, July 30). Japan's food self-sufficiency ratio hits record low. Asahi Shimbun. ⟨https://www.asahi.com/ajw/articles/14704414⟩. The Asahi Shimbun Company; 2024.
The National Bureau of Asian Research. The National Bureau of Asian Research. (2023). Decarbonizing Japan's transportation sector: Toward net-zero emissions. The National Bureau of Asian Research. ⟨https://www.nbr.org/publication/decarbonizing-japans-transportation-sector-toward-net-zero-emissions/⟩. 2023.
Thushari, I., Babel, S., 2018. Sustainable utilization of waste palm oil and sulfonated carbon catalyst derived from coconut meal residue for biodiesel production. Bioresour. Technol. 248, 199–203.
Watanabe, K., 2013. The toxicological assessment of cyclopentyl methyl ether (CPME) as a green solvent. Molecules 18, 3183–3194.
Xia, S., Tao, J., Zhao, Y., Men, Y., Chen, C., Hu, Y., et al., 2024. Application of waste derived magnetic acid-base bifunctional CoFe/biochar/CaO as an efficient catalyst for biodiesel production from waste cooking oil. Chemosphere 350, 141104.